

Cite this: DOI: 00.0000/xxxxxxxxxx

## Supplementary information: Tunable crystalline structure and electrical properties in (Pb,Sr)TiO<sub>3</sub> films grown by Liquid Phase Epitaxy<sup>†</sup>

Laura Wollesen,<sup>\*ab</sup> Paul-Antoine Douissard,<sup>a</sup> Ingrid C. Infante<sup>c</sup>, Jeremie Margueritat<sup>b</sup>, Brice Gautier<sup>c</sup>, Thierry Martin<sup>a</sup> and Christophe Dujardin<sup>\*b</sup>

Received Date  
Accepted Date

DOI: 00.0000/xxxxxxxxxx

### SEM-EDX

Table 1 gives an overview of the results from the SEM-EDX measurements performed on the studied samples and the subsequent calculations made to obtain the chemical formulas. When calculating the chemical formula of the perovskite structure (ABO<sub>3</sub>), Ti is assumed to only occupy the B-site, Pb and Sr are assumed to occupy only A-site. For the nominal values in the LPE growth melt we refer to the main article. In Figure 1 the three spectra from the SEM-EDX measurement are presented for the three Sr-containing samples.

### X-ray diffraction

In Figure 2 is the  $2\theta - \omega$  specular scans from the main article presented, but here with a logarithmic Y-scale. Besides the (H00) and (00L) peaks some low intensity satellite peaks, indicated with \*, for samples M2-Sr0.22-10  $\mu\text{m}$  and M2-Sr0.25-12  $\mu\text{m}$  are here revealed. These low intensity peaks fits with diffraction on (H0L) planes but correspond to a negligible part of the sample.

### Raman spectroscopy

For M1-17  $\mu\text{m}$  at room temperature all the observed Raman peaks can be assigned to the modes for tetragonal PTO<sup>1,2</sup>, see Figure 4 for both HV and VV configuration.

In figure 6 and Figure 5 is all recorded Raman spectra in HV

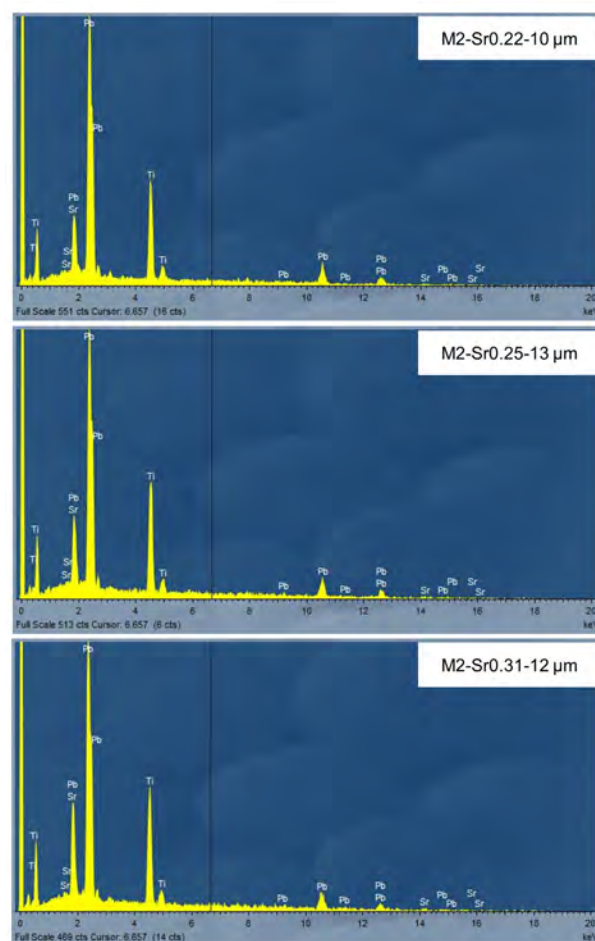


Figure S 1 SEM-EDX spectra on the Sr-containing samples. Sample references are indicated on each spectrum.

<sup>a</sup> ESRF - The European Synchrotron, 71 avenue des Martyrs 38000 Grenoble, France.

<sup>b</sup> Institut Lumière Matière, UMR5306 Université Lyon 1-CNRS, Université de Lyon, 69622 Villeurbanne cedex, France.

<sup>c</sup> Institut des Nanotechnologies de Lyon, UMR5270 Université Lyon 1-CNRS, Université de Lyon, 69621 Villeurbanne cedex, France.

<sup>†</sup> Electronic Supplementary Information (ESI) available: [details of any supplementary information available should be included here]. See DOI: 00.0000/00000000.

‡ Additional footnotes to the title and authors can be included e.g. 'Present address:' or 'These authors contributed equally to this work' as above using the symbols: ‡, §, and ¶. Please place the appropriate symbol next to the author's name and include a ¶footnotetext entry in the the correct place in the list.

Table 1 SEM-EDX. Line: Characteristic X-ray lines, wt%: weight percent, at%: atomic weight percent, Formula: chemical formula.  $\sigma$ : error at first sigma level.

Sample reference	Element	Line	wt%	$\sigma$ (wt%)	at%	$\sigma$ (at%)	Formula	$\sigma$ (Formula)
M1-17 $\mu\text{m}$								
	Ti	K-series	20.32	0.80	52.45	0.73		
	Pb	M-series	79.68	0.80	47.55	0.73		
M2-Sr0.22-10 $\mu\text{m}$								
	Ti	K-series	22.52	0.82	52.35	0.60	1	
	Sr	L-series	8.22	0.86	10.44	0.83	0.22	0.012
	Pb	M-series	69.26	1.09	37.21	0.35	0.78	0.0120
M2-Sr0.25-13 $\mu\text{m}$								
	Ti	K-series	23.47	0.84	53.13	0.59	1	
	Sr	L-series	9.57	0.90	11.84	0.82	0.25	0.012
	Pb	M-series	66.96	1.12	35.03	0.28	0.75	0.012
M2-Sr0.31-12 $\mu\text{m}$								
	Ti	K-series	22.27	0.83	50.42	0.63	1	
	Sr	L-series	12.44	0.94	15.4	0.78	0.31	0.009
	Pb	M-series	65.3	1.15	34.18	0.24	0.69	0.009

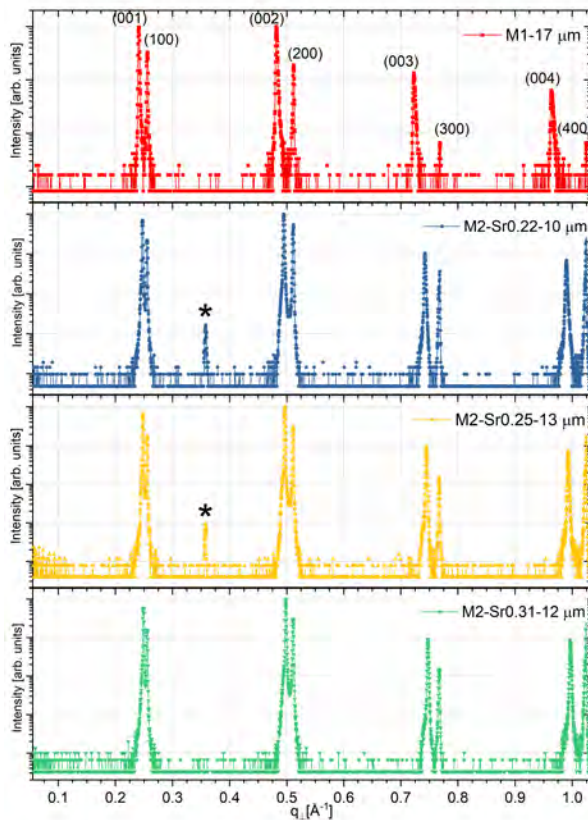


Figure S 2 X-ray diffraction  $2\theta - \omega$  specular scans with indications of (H00) and (00L) peaks for the studied samples, with  $q_{\perp} = 2/\lambda \cdot \sin(\theta)$  and  $\lambda = 1.54056 \text{ \AA}$  and Y-axis in logarithmic scale.

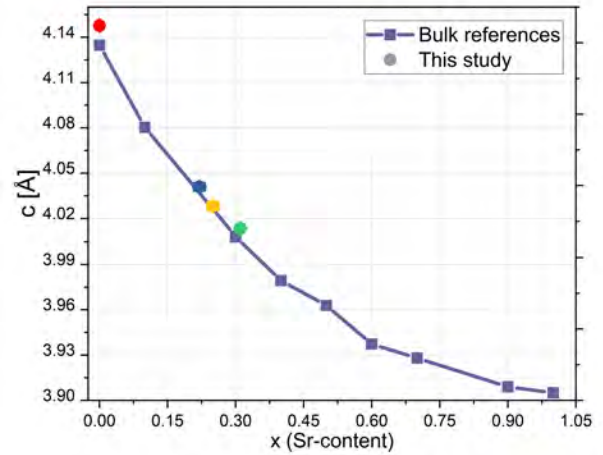


Figure S 3 The c-parameter of the investigated samples calculated from the (003) and (004)  $2\theta$  values as a function of the SEM-EDX estimated Sr-content. The error bar on the c-parameter is smaller than the symbol (difference between c parameter found by the (004) and the (003) peaks). Results compared to crystalline bulk references here included in symbols corresponding to c-parameters from  $\text{SrTiO}_3$  (00-035-0734),  $\text{Pb}_{0.1}\text{Sr}_{0.9}\text{TiO}_3$  (000570220),  $\text{Pb}_{0.3}\text{Sr}_{0.7}\text{TiO}_3$  (00-062-0320),  $\text{Pb}_{0.4}\text{Sr}_{0.6}\text{TiO}_3$  (00-062-0321),  $\text{Pb}_{0.5}\text{Sr}_{0.5}\text{TiO}_3$  (00-052-1119),  $\text{Pb}_{0.6}\text{Sr}_{0.4}\text{TiO}_3$  (00-057-0223),  $\text{Pb}_{0.7}\text{Sr}_{0.3}\text{TiO}_3$  (00-057-0222),  $\text{Pb}_{0.9}\text{Sr}_{0.1}\text{TiO}_3$  (00-057-0221) and  $\text{PbTiO}_3$  (01-070-4258)

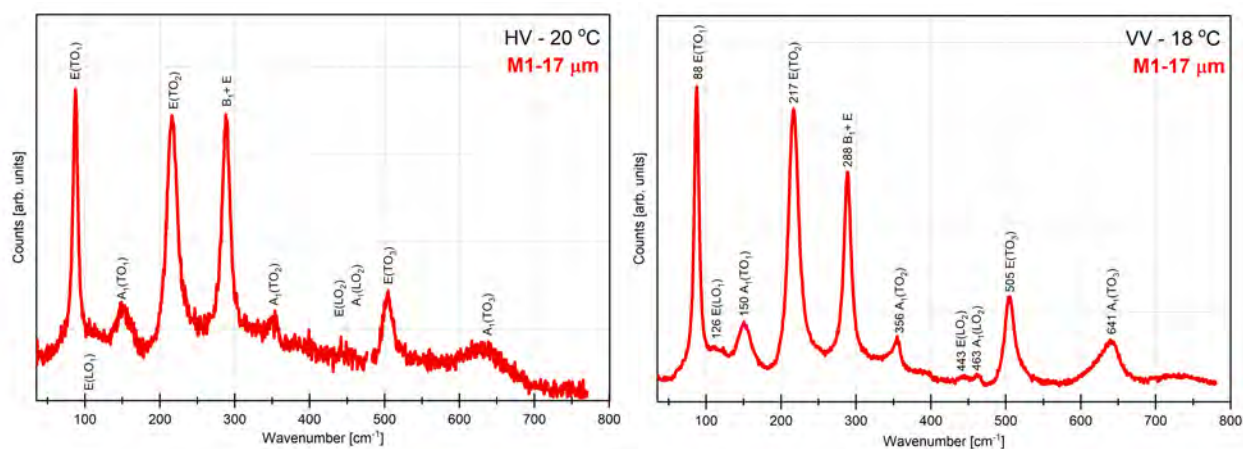


Figure S 4 Raman spectra at room temperature for M1-17  $\mu\text{m}$  in VV and HV configuration with assignment of the modes according to <sup>1,2</sup>.

and VV configuration, respectively presented as a function of temperature for the four investigated samples.

### Transmission spectra

The transmission spectra were collected using a Xenon lamp placed in an APEX illuminator (Newport). The lamp was coupled to a Cornerstone C260 monochromator with a 1200 lines/mm grating blazed at 350 nm. The transmitted beam reaches the sample with a spot size of  $\sim 3 \times 3$  mm. The transmitted intensity was measured with a 918D-UV detector (Newport) and the sample-to-detector distance is  $\sim 8$  mm. The substrates both used for growth and for reference here,  $\text{SrTiO}_3$ , is 500  $\mu\text{m}$  thick. The samples consist of a substrate with film on both sides, which is a consequence of growth by LPE.

The recorded transmission spectra are shown in Figure 7. The transmission for all the studied samples is lower than what is reported for thin films of similar compositions<sup>3-5</sup>. However, these thin films have a thickness in the range of 280-620 nm whereas the samples grown for this study are several micrometers thick. Indeed M1-13 m ( $\text{PbTiO}_3$ ) has a reduced transmission compared

to the Sr-containing samples, which are more comparable to the substrate. The different types of domains will have various transmittance and possibly scatter/deflect the light in different ways. Since the spot size of the incoming light is considerably larger than a single domain, a mix of contributions from the different types of domains in the film on both sides and the substrate contribute to the transmission spectra. Single domain transmission spectra will be the subject of a future analysis.

### Notes and references

- 1 Y. I. Yuzyuk, *Physics of the Solid State*, 2012, **54**, 1026–1059.
- 2 C. Foster, Z. Li, M. Grimsditch, S.-K. Chan and D. Lam, *Physical Review B*, 1993, **48**, 10160.
- 3 D. Ambika, V. Kumar, C. Suchand Sandeep and R. Philip, *Applied Physics B*, 2009, **97**, 661–664.
- 4 J. Yang, Y. Gao, Z. Huang, X. Meng, M. Shen, H. Yin, J. Sun and J. Chu, *Journal of Physics D: Applied Physics*, 2009, **42**, 215403.
- 5 E. Dogheche, B. Jaber and D. Rémiens, *Applied optics*, 1998, **37**, 4245–4248.

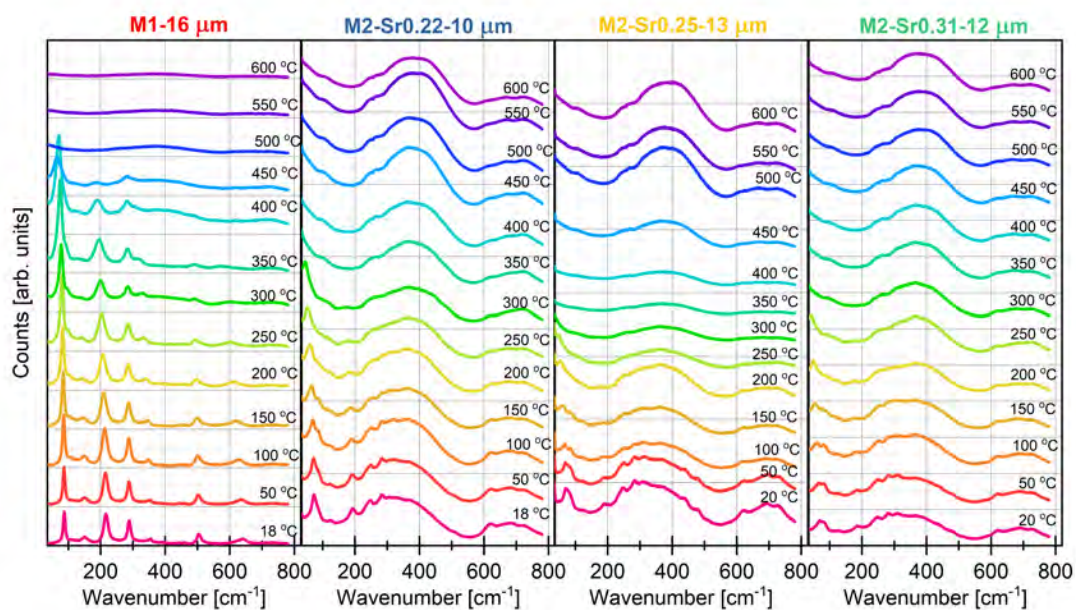


Figure S 5 All collected Raman spectra obtained in VV configuration, with the sample reference stated above each figure, at temperatures from 20 to 600  $^{\circ}\text{C}$ .

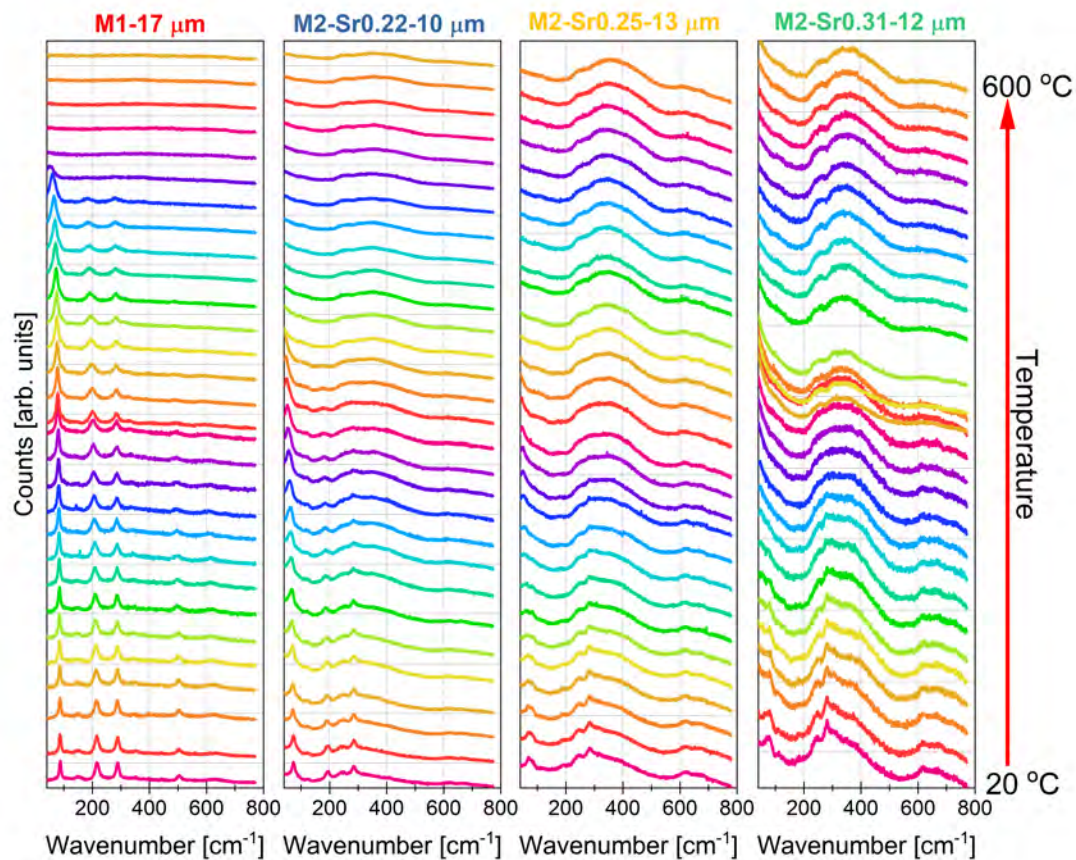


Figure S 6 All collected Raman spectra were obtained in HV configuration, with the sample reference stated above each figure, at temperatures from 20 to 600  $^{\circ}\text{C}$ .

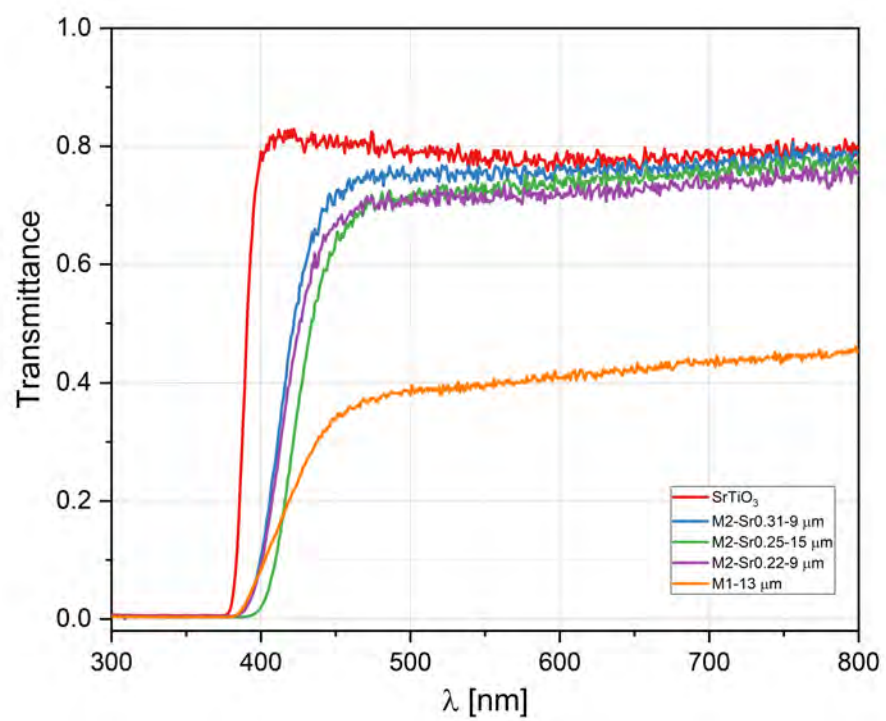


Figure S 7 Transmittance of selected samples, including a substrate. See the explanation for the sample notation in the main article.